

SI Appendix for

Sleep loss drives acetylcholine- and somatostatin interneuron-mediated gating of hippocampal activity, to inhibit memory consolidation

James Delorme¹, Lijing Wang¹, Femke Roig Kuhn², Varna Kodoth¹, Jingqun Ma³, Jessy D. Martinez¹, Frank Raven¹, Brandon A. Toth¹, Vinodh Balendran¹, Alexis Vega Medina¹, Sha Jiang¹, Sara J. Aton^{1#}

¹ Department of Molecular, Cellular, and Developmental Biology, University of Michigan, Ann Arbor, MI 48019

² Program in Behavioural and Cognitive Neurosciences, University of Groningen, 9700 AB Groningen, the Netherlands

³ Bioinformatics Core, University of Michigan Biomedical Research Core Facilities, Ann Arbor, MI 48019

This PDF file includes:

SI Materials and Methods
SI Figure Legends
Figures S1 to S7

Other SI materials for this manuscript include the following:

Datasets S1 – S3

SI Materials and Methods

Mouse husbandry, handling, and behavioral procedures

All animal husbandry and experimental procedures were approved by the University of Michigan Institutional Animal Care and Use Committee (PHS Animal Welfare Assurance number D16-00072 [A3114-01]). Mice were maintained on a 12 h:12 h light:dark cycle with *ad lib* access to food and water. For behavioral experiments, 3-4 month old C57Bl6/J mice (Jackson) or transgenic mice on a C57Bl6 background (see below) were individually housed with beneficial enrichment one week prior to experimental procedures, and were habituated to experimenter handling (5 min/day) for five days prior to experimental procedures. At lights on (ZT0), animals were either left in their home cage (HC) or underwent single-trial contextual fear conditioning (CFC). During CFC, mice were placed in a novel conditioning chamber (Med Associates), and were allowed to explore the chamber freely for 2.5 min, after which they received a 2-s, 0.75 mA foot shock through the chamber's grid floor. Mice remained in their conditioning chamber for an additional 28 s, after which they were then returned to their home cage. Mice were then either permitted *ad lib* sleep (Sleep) or were sleep-deprived (SD) by gentle handling (1, 2) over the next 3-5 h for immunohistochemical or biochemical studies as described below. For behavioral studies of CFM consolidation, SD occurred over 6 h (from ZT0-6). Gentle handling procedures included interruption of sleep attempts (i.e., cessation of movement and assumption of stereotyped sleep postures in the nest) with cage tapping or shaking, or nest disturbance. Sleep was verified and quantified in individual mice in *ad lib* sleep conditions based on absence of movement and maintenance of stereotyped (crouched) sleep postures, consistent with our prior studies (3).

For behavioral analysis of CFM (with or without pharmacogenetic manipulations described below; shown in **Figure 1** and **Figures 5-8**) mice of the appropriate genotypes from the same litter were randomly assigned to experimental and control groups. All mice underwent single-trial CFC as described above, followed by either *ad lib* sleep or 6 h SD (a length of time sufficient for disruption of CFM (2, 4, 5)) and subsequent recovery sleep. CFM was assessed behaviorally 24 h after CFC as described below.

Translating Ribosome Affinity Purification (TRAP)

For pS6 RNA-sequencing (TRAP-seq) experiments, 3-4 month old C57Bl/6J mice were randomly assigned to one of four groups: HC + Sleep ($n = 8$), HC + SD ($n = 7$), CFC + Sleep ($n = 8$), CFC + SD ($n = 7$). Beginning at ZT3, animals were euthanized with an i.p injection of pentobarbital (Euthasol) and hippocampi were dissected in cold dissection buffer (1x HBSS, 2.5 mM HEPES [pH 7.4], 4 mM NaHCO₃, 35 mM glucose, 100µg/ml cycloheximide). Hippocampal tissue was then transferred to a glass dounce homogenizer containing homogenization buffer (10 mM HEPES [pH 7.4], 150 mM KCl, 10 mM MgCl₂, 2 mM DTT, cOmplete™ Protease Inhibitor Cocktail [Sigma-Aldrich, 11836170001], 100 U/mL RNasin® Ribonuclease Inhibitors [Promega, N2111], and 100 µg/mL cycloheximide) and manually homogenized on ice. Homogenate was transferred to 1.5 ml LoBind tubes (Eppendorf) and centrifuged at 4°C at 1000 g for 10 min. The resulting supernatant was transferred to a new tube, and 10% NP40 was added to the samples (90 µL), and incubated 5 min on ice. Samples were centrifuged at 4°C at maximum speed for 10 min, 500 µL supernatant transferred to a new LoBind tube, and incubated with anti-pS6 244-247 (ThermoFisher 44-923G)(6). Antibody binding of the homogenate-antibody solution occurred over 1.5 h at 4°C with constant rotation. For affinity purification, 200 µl of Protein G Dynabeads (ThermoFisher, 10009D) were washed 3 times in 0.15M KCl IP buffer (10 mM HEPES [pH 7.4], 150 mM KCl, 10 mM MgCl₂, 1% NP-40) and incubated in supplemented homogenization buffer (+10% NP-40). Following this step, supplemented buffer was removed, homogenate-antibody solution was added directly to the Dynabeads, and the solution was incubated for 1 h at 4°C with constant rotation. After incubation, the RNA-bound beads were washed four times in 900µL of 0.35M KCl (10mM HEPES [pH 7.4], 350 mM KCl, 10 mM MgCl₂, 1% NP40, 2 mM DTT, 100 U/mL RNasin® Ribonuclease Inhibitors [Promega, N2111], and 100 µg/mL cycloheximide). During the final wash, beads were placed onto the magnet and moved to room temperature. After removing the supernatant, RNA was eluted by vortexing the beads vigorously in 350 µl RLT (Qiagen, 79216). Eluted RNA was purified using RNeasy Micro kit (Qiagen).

Sst::RiboTag mice were generated by crossing *SST-IRES-CRE* (B6N.Cg-Sst^{tm2.1(SST-cre)Zjh}; Jackson) mice to the *RiboTag^{fl/fl}* (B6N.129-Rpl22^{tm1.1Psam}/J; Jackson) mouse line to generate mice expressing HA-tagged Rpl22 protein in *Sst*+ interneurons. For *Sst*-TRAP, ribosomes and associated transcripts were affinity purified by incubating homogenate with 1/40 (10 µl) anti-HA antibody (Abcam, ab9110) (7).

RNA sequencing and data analysis

RNA-seq was carried out at the University of Michigan's DNA sequencing core. cDNA libraries were prepared by the core using Takara's SMART-seq v4 Ultra Low Input RNA Kit (Takara 634888) and sequenced on Illumina's NovaSeq 6000 platform. Sequencing reads (50 bp, paired end) were mapped to *Mus musculus* using Star v2.6.1a and quality checked with Multiqc(v1.6a0). Reads mapped to unique transcripts were counted with featureCounts (8). For weighted gene co-expression network analysis (WGCNA) analysis, raw counts for pS6 data was filtered to keep genes with at least 30 total reads across the 30 samples. The filtered reads were normalized using the DESeq2 variance stabilizing transformation (vst) function (9), and were filtered to keep only genes with a variance larger than 0.03 among the 30 samples (i.e., those with informative variability between samples) in order to optimize use of computational resources. The 1662 genes were retained and used for the network analysis in WGCNA (10).

For cell type-specific expression analysis (CSEA), genes from the Brown and Magenta clusters were combined and uploaded into the CSEA Tool (<http://genetics.wustl.edu/jdlab/csea-tool-2/>), selecting Candidate Gene List from: Mice (11). Cell type-specific (TRAP) expression data used by this tool were originally detailed in (12-16) as described in (11). Results for cell types enriched in our pS6 clusters were analyzed at the most stringent specificity index ($pSI < 0.0001$). Observing significant values in cholinergic (+Chat), orexinergic (Hcrt+), and GABAergic (Pnoc+, Cort+) neurons, we plotted genes from the highest and second highest specificity index. To analyze how SD promotes pS6 enrichment of these cell type-specific transcripts, we calculated the Log₂FC values of combined CFC and HC mice and assessed the effect of SD over sleep control mice (9).

Quantitative PCR (qPCR)

RNA from TRAP experiments was quantified by spectrophotometry (Nanodrop Lite, ThermoFisher). 50ng of RNA was reverse transcribed using iScript cDNA Synthesis (Bio-Rad, Catalog: 1708890) or SuperScript IV Vilo Master Mix (Invitrogen, Catalog: 11756060). qPCR was performed on diluted cDNA that employed either Power SYBR Green PCR Mix (Invitrogen 4367659) or TaqMan Fast Advanced Master Mix (Invitrogen, Catalog: 4444557). Primers were designed using Primer3(v. 0.4.0) and confirmed with NCBI primer Basic Local Alignment Search Tool (BLAST). qPCR reactions were

measured using a CFX96 Real-Time System, in 96-well reaction plates (Bio-Rad). For pS6- and Sst-TRAP experiments, housekeeping genes for data normalization were determined by assessing the stability values prior to analysis (17). Analyses compared *Pgk1*, *Gapdh*, *Actg1*, *Tuba4a*, *Tbp*, and *Hprt*. Results from both analyses independently found *Gapdh* and *Pgk1* to be the most stable and least altered housekeeping transcripts following SD or CFC. Therefore expression was normalized to the geometric mean of *Gapdh* and *Pgk1*. To assess differences in transcript abundance between groups, values were expressed as fold changes normalized to the mean values for mice in the HC + Sleep group. To measure relative enrichment of mRNA in pS6-TRAP or Sst-TRAP experiments, each sample was normalized to the geometric mean of *Pgk1* and *Gapdh* housekeeping transcripts and then normalized to the corresponding Input sample (TRAP Enrichment = $2^{(\Delta Ct_{target} - \Delta Ct_{housekeeping})}$).

Immunohistochemistry and protein expression analysis

Mice were injected with euthasol and perfused with cold 1xPBS followed by 4% paraformaldehyde. Brains were extracted and submerged in ice-cold fixative for 24hrs and transferred to 30% sucrose solubilized in 1xPBS. 50µm-thick coronal sections were cut on a cryostat. Tissue was blocked for 2-hours in 1% NGS and 0.3% Triton X-100 followed by 2-3 days of 4°C incubation in 1xPBS (5% NGS, 0.3% Triton X-100) with primary antibody(ies): pS6 S235-236 (Cell Signaling, Catalog: 4858, 1:500), pS6 S244-247(ThermoFisher, Catalog: 44-923G, 1:500), Sst (Millipore, MAB354, 1:200), Pvalb (Synaptic Systems, Catalog: 195004, 1:500), cFos (Abcam, Catalog: 190289, 1:500), Arc (Synaptic Systems, 156004, 1:500) by constant rotation. Sections were then washed 3x in 1xPBS (1% NGS, 0.2% Triton X-100) and incubated for 1hr in 1xPBS (5% NGS, 0.3% TX-100) and secondary antibody: Fluorescein (FITC) AffiniPure Goat Anti-Rabbit IgG (Jackson, Catalog: 111-095-003, 1:200), Donkey anti-Rat IgG Alexa Fluor 488 (ThermoFisher, A-21208), Goat Anti-Guinea Pig IgG Alexa Fluor 555 (Abcam, Catalog: ab150186, 1:200), Goat anti-Rabbit IgG Alexa Fluor 633 (ThermoFisher, Catalog: A-21070, 1:200). Tissue was then washed 3x in 1xPBS (1% NGS, 0.2% Triton X-100), 3x in 1xPBS, and then mounted on coverslips and embedded in ProLong Gold Antifade Mountant (ThermoFisher, Catalog: P10144).

For optical density (OD) calculations, 4 fluorescent microscope images were taken from each brain and analyzed in Fiji. A scorer blind to experimental condition collected

optical density values from CA1 and CA3 pyramidal cell layers as well as background. For analysis, equally sized regions of interest (ROIs) were obtained for each image. OD values were background subtracted and normalized to HC + Sleep control groups. For DG cell counts, pS6 co-localization, and Sst and Pvalb quantification, images were captured using a 20x objective lens on a Leica SP5 laser scanning confocal microscope. Z-projected images were analyzed in MIPAR image analysis software in their raw grayscale format (18) For DG cell counts, a non-local means filter was used to reduce image noise and an adaptive threshold applied to identify cell counts whose mean intensity values were 200% its surroundings. Colocalization and mean fluorescence intensity were determined by adaptive thresholding of fluorescent signals, quantifying percentage overlap of ROI obtained from both signals and mean fluorescent intensity values of underlying fluorescent signals.

AAV virus injections, pharmacogenetic manipulations, and CFM testing

At age 3-4 months, male *SST-IRES-CRE* (B6N.Cg-Sst^{tm2.1(SST-cre)}Zjh) or *Chat-CRE* (B6.FVB(Cg)-Tg(Chat-cre)GM53Gsat/Mmucd, MMRRC) mice underwent bilateral dorsal hippocampus or MS viral transduction. For pharmacogenetic activation, mice were transduced with either hM3dq-mCherry (pAAV-hSyn-DIO-hM3D(Gq)-mCherry, University of Pennsylvania Vector Core, Lot: V55836) or (as a control) an mCherry reporter (EF1A-DIO-mCherry, University of Pennsylvania Vector Core, Lot: PBK273-9). For pharmacogenetic inhibition, mice were transduced with hM4Di-mCitrine (AAV8 hSyn-DIO-HA-hM4D(Gi)-P2a-Citrine, University of Pennsylvania Vector Core, Lot: PBK399-9) or (as a control) a YFP reporter (pAAV-Ef1a-DIO EYFP, Addgene). For transduction of *SST-IRES-CRE* mice, 1 μ l of virus was injected using a 33-gauge beveled syringe needle into the dorsal hippocampus each hemisphere at a rate of 4 nL/s (2.1 mm posterior, 1.6 mm lateral, 2.1 mm ventral to Bregma). For transduction of *Chat-CRE* mice, 1 μ l of virus was injected into the medial septum (0.75 mm anterior, 0.0 mm lateral, 4.0 mm ventral to Bregma). For behavioral studies shown separately in **Figures 5-8** and **Supplementary Figure S7**, mice from individual litters were randomly assigned to experimental and treatment groups.

After 2-4 weeks of postoperative recovery and daily handling as described above, mice underwent single-trial CFC at ZT0. Immediately after CFC, mice were injected i.p. with either 3 mg/kg clozapine N-oxide (CNO; Tocris, Catalog: 4936, Lot: 13D/233085) in

0.5% DMSO and saline, or 0.5% DMSO vehicle (VEH). All mice were then returned to their home cage for *ad lib* sleep (or 6-h SD, for experiments shown in **Figure S7**). Over the first 30-60 min following administration of CNO or VEH, all mice were observed for apparent changes in sleep behavior, behavioral state, or locomotor activity; none were observed in any treatment group, consistent with previously published data (19). Across SD (**Figure S7**), the number of interventions required to sustain wakefulness (e.g., cage taps, cage shakes, nest disturbances) were recorded. No significant differences were found in the number of interventions of each type required for SD between hM4Di-expressing and control mice ($p > 0.45$ for all comparisons, Students t-test), suggesting that sleep drive did not differ as a function of pharmacogenetic manipulation.

Mice were returned to the CFC context 24 h following CFC, for 5 min of video monitoring. Context-specific freezing behavior was quantified by a scorer blinded to experimental conditions as described previously (2, 20, 21) as a measure of CFM. For all statistical comparisons, freezing amounts during CFM testing were quantified as % of the 5-min recording period. Baseline % freezing during CFC (prior to foot shock) was subtracted % freezing during testing to quantify changes in freezing due to CFM. To verify effects of pharmacogenetic manipulations on the hippocampal network, 2 weeks following CFM tests, mice were administered CNO (or VEH) at lights on, and were allowed 3 h *ad lib sleep* prior to perfusion for immunohistochemical analysis of activity-dependent cFos expression or S6 phosphorylation.

SI Figure Legends

Figure S1. CFC-driven increases in hippocampal pS6 expression. *Top:* CFC (at ZT0) increased the number of pS6+ (S244-247) DG neurons at ZT0.5 h ($p < 0.05$, Holm-Sidak *post hoc* test) and ZT3 ($p < 0.001$, Holm-Sidak *post hoc* test). Both HC and CFC mice had greater numbers of pS6+ neurons at ZT3 (two-way ANOVA: main effect of time, $F = 50.63$, $p < 0.001$; main effect of CFC, $F = 33.59$, $p < 0.001$; time \times CFC interaction, *N.S.*), likely reflecting the effect of sleep time between the time points. *Bottom:* pS6 expression was unchanged by CFC in CA1 and CA3 pyramidal regions.

Figure S2. SD increases S6 phosphorylation in the neocortex. pS6 (S235-236 and S244-247) expression in neocortical regions dorsal hippocampus (i.e., primary somatosensory cortex). SD increased the numbers of pS6+ neurons using antibodies targeting pS6 S235-236 ($p < 0.0001$, Student's t-test) and S244-247 ($p < 0.01$).

Figure S3. Scatter plot of Brown/Magenta cluster eigengenes and *Sst*, *Npy*, and *Crh* with proportional time spent in sleep (of 3 h prior to sacrifice) for individual mice. R and p values from Pearson correlation shown.

Figure S4. Whole hippocampus gene expression following 3 h SD or *ad lib* sleep. qPCR data for activity-dependent, GABAergic, and CSEA-predicted transcripts in whole hippocampus (Input) following 3h of SD ($n = 4$; red triangles) or Sleep ($n = 5$; blue circles). Sleep vs SD, ***, **, and * indicated $p < 0.001$, $p < 0.01$, and $p < 0.05$, respectively, Student's t-test.

Figure S5. Mean *Sst* and *Pvalb* fluorescence intensity values in DG after sleep vs. SD. Mean fluorescence intensity values for *Sst*+ and *Pvalb*+ interneurons (numeric values indicate mean numbers of neurons quantified per animal) in DG following 3 h of *ad lib* sleep ($n = 5$ mice) or SD ($n = 5$ mice). 3-h SD reduced *Sst* staining intensity in DG neurons (Student's t-test, $p < 0.01$).

Figure S6. Viral transduction of dorsal hippocampus *Sst*+ interneurons. AAV-driven expression of mCherry in *Sst*+ interneurons was restricted to dorsal hippocampus

(primarily DG and CA1) and a small region of overlying neocortex, corresponding to the injection needle tract. Scale bar = 500 μ m.

Figure S7. Pharmacogenetic inhibition of Sst+ interneurons or MS cholinergic neurons during SD does not fully rescue CFM consolidation. **A) Top:** Experimental design: *SST-IRES-CRE* mice expressing YFP ($n = 12$) or hM4Di-mCitrine ($n = 15$) in dorsal hippocampus underwent single-trial CFC at lights on, and then were immediately administered CNO (3 mg/kg, i.p.) and were sleep-deprived (SD) for the next 6 h in their home cage. 24 h later, after recovery *ad lib* sleep, all mice were returned to the CFC context for assessment of contextual fear memory (CFM). **Bottom:** Sleep-deprived hM4Di-expressing mice did not show significantly greater CFM consolidation (measured as % time freezing) after 24 h, compared with YFP control mice ($p = 0.27$, Student's t-test). **B) Top:** Experimental design: *Chat-CRE* mice expressing YFP ($n = 7$) or hM4Di-mCitrine ($n = 7$) in MS underwent single-trial CFC at lights on, and then were immediately administered CNO (3 mg/kg, i.p.) followed by 6-h SD. CFM was assessed 24 h later, after recovery *ad lib* sleep). **Bottom:** hM4Di-expressing mice did not show significantly greater CFM consolidation (measured as % time freezing) after 24 h, compared with control mice ($p = 0.21$, Student's t-test).

Dataset S1 – WGCNA cluster genes and CSEA analysis

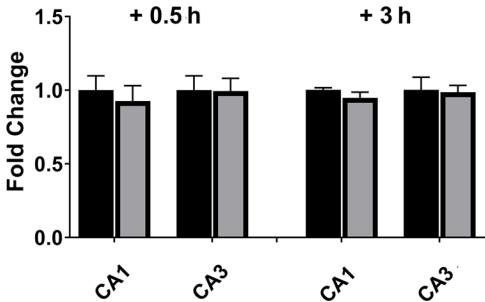
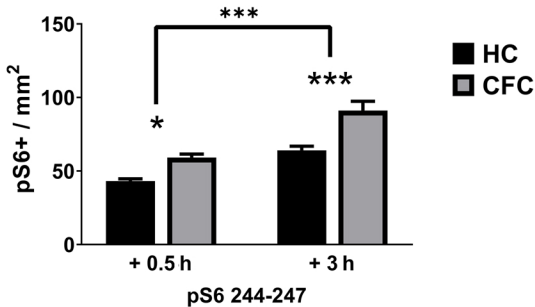
Dataset S2 – kWithin for all genes in WGCNA analysis, and for genes within each cluster

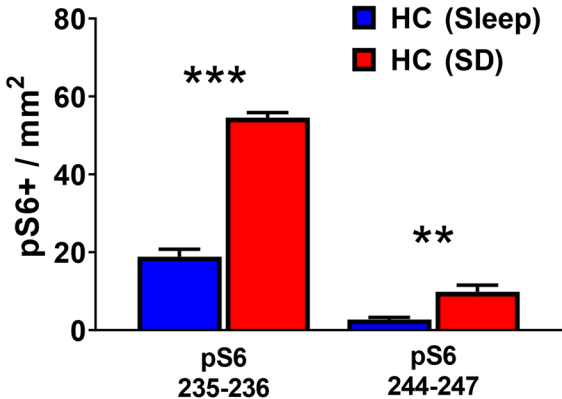
Dataset S3 – Summary of qPCR results for RNAs measured in both pS6-TRAP and SST-TRAP

References cited

1. Durkin J, *et al.* (2017) Cortically coordinated NREM thalamocortical oscillations play an essential, instructive role in visual system plasticity. *Proceedings National Academy of Sciences* 114(39):10485-10490.
2. Ognjanovski N, Broussard C, Zochowski M, & Aton SJ (2018) Hippocampal Network Oscillations Rescue Memory Consolidation Deficits Caused by Sleep Loss. *Cereb. Cortex* 28(10):3711-3723.
3. Delorme JE, Kodoth V, & Aton SJ (2019) Sleep loss disrupts Arc expression in dentate gyrus neurons. *Neurobiol Learn Mem* 160:73-82.
4. Vecsey CG, *et al.* (2009) Sleep deprivation impairs cAMP signalling in the hippocampus. *Nature* 461(7267):1122-1125.
5. Graves LA, Heller EA, Pack AI, & Abel T (2003) Sleep deprivation selectively impairs memory consolidation for contextual fear conditioning. *Learn. Mem.* 10(3):168-176.
6. Knight ZA, *et al.* (2012) Molecular profiling of activated neurons by phosphorylated ribosome capture. *Cell* 151(5):1126-1137.
7. Shigeoka T, Jung J, Holt CE, & Jung H (2018) Axon-TRAP-RiboTag: Affinity Purification of Translated mRNAs from Neuronal Axons in Mouse In Vivo. *RNA Detection (Methods in Molecular Biology)*, (Humana Press, New York), pp 85-94.
8. Liao Y, Smyth GK, & Shi W (2014) featureCounts: An Efficient General Purpose Program for Assigning Sequence Reads to Genomic Features *Bioinformatics* 30(7):329-330.
9. Love MI, Huber W, & Anders S (2014) Moderated estimation of fold change and dispersion for RNA-seq data with DESeq2. *Genome Biology* 15.
10. Langfelder P & Horvath S (2008) WGCNA: an R package for weighted correlation network analysis. *BMC Bioinformatics* 9.
11. Xu X, Wells AB, O'Brien DR, Nehorai A, & Dougherty JD (2014) Cell Type-Specific Expression Analysis to Identify Putative Cellular Mechanisms for Neurogenetic Disorders. *J Neurosci* 34(4):1420-1431.
12. Doyle JP, *et al.* (2008) Application of a Translational Profiling Approach for the Comparative Analysis of CNS Cell Types. *Cell* 135(4):749-762.
13. Dougherty JD, *et al.* (2012) Candidate pathways for promoting differentiation or quiescence of oligodendrocyte progenitor-like cells in glioma *Cancer Research* 72(18):4856-4868.
14. Dougherty JD, *et al.* (2013) The disruption of Celf6, a gene identified by translational profiling of serotonergic neurons, results in autism-related behaviors *J Neurosci* 33(7):2732-2753.
15. Dalal J, *et al.* (2013) Translational profiling of hypocretin neurons identifies candidate molecules for sleep regulation. *Genes Development* 27(5):565-578.
16. Gorlich A, *et al.* (2013) Reexposure to nicotine during withdrawal increases the pacemaking activity of cholinergic habenular neurons. *Proc Natl Acad Sci USA* 110(42):17077-17082.

17. Andersen CL, Jensen JL, & Orntoft TF (2004) Normalization of Real-Time Quantitative Reverse Transcription-PCR Data: A Model-Based Variance Estimation Approach to Identify Genes Suited for Normalization, Applied to Bladder and Colon Cancer Data Sets. *Cancer Research* 64:5245-5250.
18. Sosa JM, Huber DE, Welk B, & H.L. F (2014) Development and application of MIPAR™: a novel software package for two- and three-dimensional microstructural characterization. *Integrating Materials and Manufacturing Innovation* 3:123-140.
19. Gerashchenko D, Salin-Pascual R, & Shiromani PJ (2001) Effects of hypocretin-saporin injections into the medial septum on sleep and hippocampal theta. *Brain Res* 913(1):106-115.
20. Ognjanovski N, *et al.* (2017) Parvalbumin-expressing interneurons coordinate hippocampal network dynamics required for memory consolidation. *Nature Communications* 8:15039.
21. Ognjanovski N, Maruyama D, Lashner N, Zochowski M, & Aton SJ (2014) CA1 hippocampal network activity changes during sleep-dependent memory consolidation. *Front Syst Neurosci* 8:61.

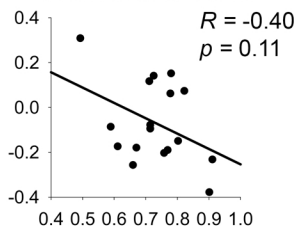
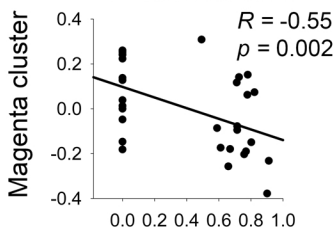
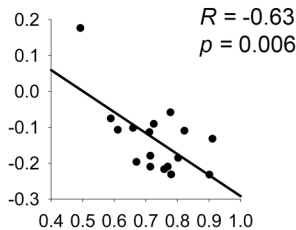
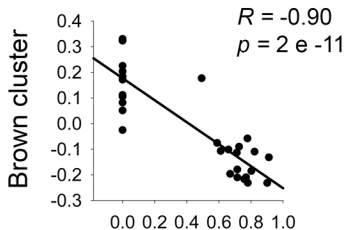




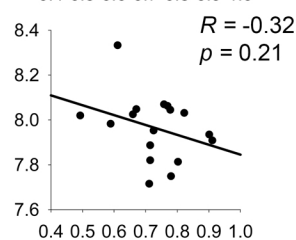
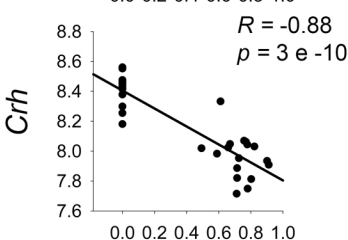
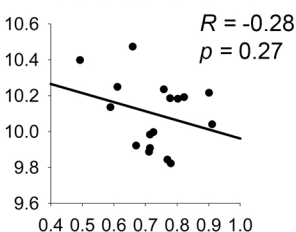
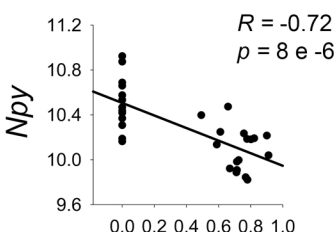
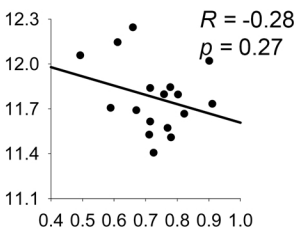
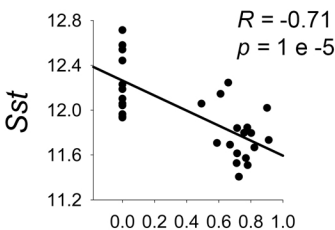
Including SD:

Sleep only:

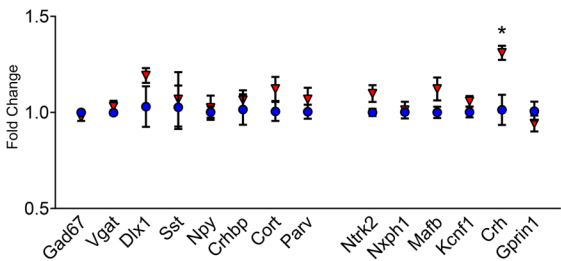
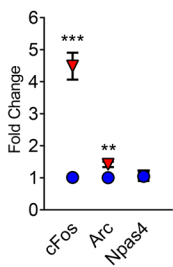
Eigengene expression



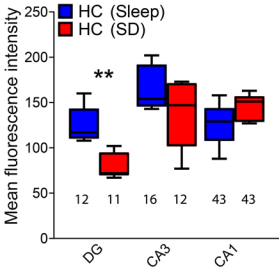
RNA expression level



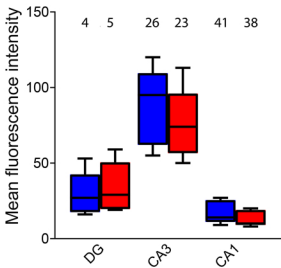
Proportion time spent in sleep (3 h)

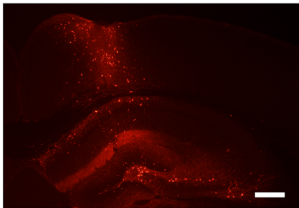
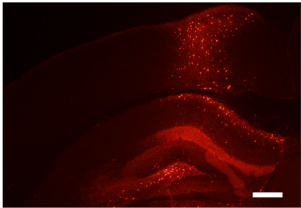


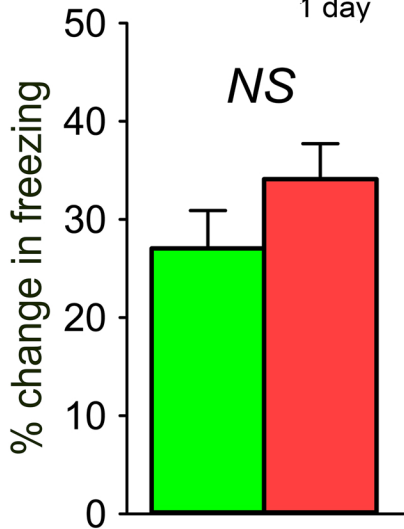
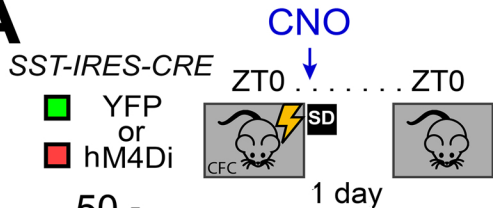
Sst



Pvalb





A**B**